Determinants of the Translational Mobility of a Small Solute in Cell Cytoplasm

H. Pin Kao, James R. Abney, and A. S. Verkman

Departments of Medicine and Physiology, Cardiovascular Research Institute, University of California, San Francisco, California 94143-0532

Abstract. The purposes of this study were: (*a*) to measure the translational mobility of a small solute in cell cytoplasm; (*b*) to define quantitatively the factors that determine solute translation; and (*c*) to compare and contrast solute rotation and translation. A small fluorescent probe, 2,7-bis-(2-carboxyethyl)-5-(and 6-)-carboxyfluorescein (BCECF), was introduced into the cytoplasm of Swiss 3T3 fibroblasts. BCECF translation was measured by fluorescence recovery after photobleaching; rotation was measured by Fourier transform polarization microscopy. Diffusion coefficients relative to those in water (D/D_0) were determined by comparing mobility in cytoplasm with mobility in standard solutions of known viscosity. At isosmotic cell volume, the relative diffusion coefficients for BCECF translation and rotation in cytoplasm were 0.27 ± 0.01 (SEM, n = 24, 23°C) and 0.78 ± 0.03 (n = 4), respectively. As cell volume increased from 0.33 to 2 times isosmotic volume, the relative translational diffusion coefficient increased from 0.047 to 0.32, while the relative rotational diffusion coefficient remained constant. The factors determining BCECF translation were evaluated by comparing rotation and translation in cytoplasm, and in artificial solutions containing dextrans (mobile barriers) and agarose gels (immobile barriers). It was concluded that the hindrance of BCECF translation in cytoplasm could be quantitatively attributed to three independent factors: (*a*) fluid-phase cytoplasmic viscosity is 28% greater than the viscosity of water (factor 1 = 0.78); (*b*) 19% of BCECF is transiently bound to intracellular components of low mobility (factor 2 = 0.81); and most importantly, (*c*) translation of unbound BCECF is hindered 2.5-fold by collisions with cell solids comprising 13% of isosmotic cell volume (factor 3 = 0.40). The product of the 3 factors is 0.25 ± 0.03, in good agreement with the measured D/D_0 of 0.27 ± 0.01. These results provide the first measurement of the translational mobility of a small solute in cell cytoplasm and define quantitatively the factors that slow solute translation.

CELL cytoplasm is a complex non-Newtonian fluid comprising an aqueous fluid-phase filling the space within an entangled mesh of filamentous skeletal proteins (cytomatrix) and other macromolecular structures (Bridgman and Reese, 1984; Clegg, 1984; Fulton, 1982; Gershon et al., 1985; Keith, 1973; Mastro and Keith, 1984; Porter, 1984). The factors that determine the rotation and translation of solute molecules within this crowded milieu have been the topic of considerable recent interest due to their probable impact on the rates of metabolic reactions. At least three cytoplasmic factors will contribute to solute mobility: (*a*) fluid-phase cytoplasmic viscosity, i.e., the viscosity in the aqueous space between macromolecules; (*b*) solute binding to macromolecular structures; and (*c*) collisional (direct plus hydrodynamic) interactions between the solute and macromolecular obstacles. The relative contributions of these three factors will depend on solute size and the type and extent of solute motion. In this study we focus primarily on the long (relative to the characteristic macromolecular spacing) range translation of small solutes. Such motion plays a role in many cellular processes, including the translocation of cyclic nucleotides in signal transduction, the vectorial transport of solutes across epithelial cells, and the movement of nucleic acids from the cytoplasm to the nucleus for replication and transcription. The translational diffusion of a small solute in cell cytoplasm has not been measured previously by FRAP.

Most studies of dynamics in the cytoplasm have focused on measurement of a single parameter that reflects how rapidly molecules rotate or translate. These measurements thus yield "apparent" cytoplasmic viscosities, which reflect all impediments to motion: the true fluid-phase viscosity, the effects of binding, and the effects of collisions. When the rotational mobility of small molecules in the cytoplasm is characterized in this fashion using electron spin resonance (Keith et al., 1977; Lepock et al., 1983; Mastro et al., 1984) or steady-state fluorescence anisotropy techniques (Dix and Verkman, 1990; Lindmo and Steen, 1977), apparent rotational viscosities in the range 2 to 20 cP (water is 1 cP) are obtained. Similarly, when translational mobilities are characterized via direct observation of the diffusion of microinjected dyes, electron spin resonance, or FRAP, appar-

ent translational viscosities are found to lie in the same range (Jacobson and Wojcieszyn, 1984; Kreis et al., 1982; Luby-Phelps et al., 1986, 1987, 1988; Wojcieszyn et al., 1981). The interpretation of these values is subject to several caveats. First, the electron spin resonance results are based on an uncertain estimate of intracellular probe concentration, while the FRAP results are based on an extrapolation of data obtained from probes of different molecular size to zero size. Second, and more importantly, none of these results provide quantitative information about the individual factors contributing to the measured viscosity.

We recently introduced a method of determining fluid-phase viscosity (microfluorimetric measurement of picosecond anisotropy decay; Fushimi and Verkman, 1991) that overcomes many of the limitations in previous measurements of solute mobility in cells. The data yield the rotational mobilities of bound and unbound probe, as well as the fraction of probe in each state. These measurements revealed that a significant (15–30%) fraction of fluorophores bind to relatively immobile cellular components. More importantly, it was demonstrated that the fluid-phase cytoplasmic viscosity sensed by the unbound probe was in the range 1.2–1.4 cP for several small fluorophores in Swiss 3T3 fibroblasts (Fushimi and Verkman, 1991) and several types of kidney epithelial cells (Periasamy et al., 1992). This is a surprisingly low viscosity, suggesting that the physical properties of aqueous domain cell cytoplasm are similar to those of water.

The purposes of the present study are: (*a*) to measure the translational mobility of a small solute in cell cytoplasm; (*b*) to define quantitatively the factors that determine solute translational mobility; and (*c*) to compare the rotation and translation of probes in the cytoplasm. A FRAP apparatus was constructed and data analysis methods were developed for quantitative determination of the translational mobilities of small molecules that diffuse rapidly in cell cytoplasm. It was found that the translational diffusion of a small fluorescent probe was approximately four times slower in cell cytoplasm than in water. It is shown that this inhibition of translational diffusion arises because fluid-phase cytoplasmic viscosity is slightly higher than the viscosity of water, a small amount of probe binds to intracellular structures, and, most significantly, because the probe collides with intracellular structures.

Materials and Methods

Cell Culture and Labeling

Swiss 3T3 fibroblasts (No. CL-101; American Type Collection, Rockville, MD) were grown on 18-mm diameter round glass coverslips in DME-H21 supplemented with 5% FCS, 100 U/ml penicillin, and 100 μg/ml streptomycin. Cells were maintained at 37°C in a 95% air/5% CO_2 incubator and used before cells had attained confluence. Cells were labeled with 2,7-bis-(2-carboxyethyl)-5-(and 6-)carboxyfluorescein (BCECF)[1] by a 10-min incubation with 5 μM BCECF-AM (acetoxylmethylester; Molecular Probes, Junction City, OR) at 37°C in PBS (138 mM NaCl, 2.7 mM KCl, 0.7 mM $CaCl_2$, 1.1 mM $MgCl_2$, 1.5 mM KH_2PO_4, 8.1 mM Na_2HPO_4, 5 mM glucose, pH 7.4). Cells were then washed and incubated for an additional 15–30 min at 37°C in buffer not containing BCECF-AM to facilitate intracellular deesterification. Coverglasses containing BCECF-loaded cells were transferred to a 200-μl perfusion chamber (to facilitate buffer changes) in which the cell-free surface of the coverglass was accessible to a nonimmersion objective or a short-working-distance immersion objective (Chao et al., 1989). All experiments were carried out at 23°C.

FRAP Apparatus

A FRAP apparatus was constructed to resolve recovery half-times down to 5 ms (Fig. 1). Cells were illuminated with a Gaussian-profile beam (488 nm) from a CR-4 Ar laser (Coherent, Inc., Palo Alto, CA) focused to a 3-μm radius spot through a 16× quartz objective (E. Leitz, Rockleigh, NJ, numerical aperture 0.25) on an inverted epifluorescence microscope. To photobleach the sample, an unattenuated laser pulse (4–5 × 10^3 times more intense than the probe beam) of 2–3 ms duration was generated using a rapid shutter (Uniblitz, model T132; Vincent Associates, Rochester, NY). To monitor prebleach and postbleach fluorescence, an attenuated probe beam was formed by reflections off of two glass wedge prisms and two front-surfaced mirrors; a neutral density filter (1.8 OD U) was positioned between the mirrors to set the attenuation ratio. The mirrors and wedge prisms were mounted on two-axis micropositioners to facilitate alignment of the unattenuated and attenuated beams. Emitted fluorescence passed through a 510-nm dichroic mirror, GG515 barrier filter, and rapid shutter (to protect the photomultiplier during the photobleaching pulse; model D122; Uniblitz), and was detected by an R928 photomultiplier (Hamamatsu, Middlesex, NJ) operating at 500–900 V. Photomultiplier signals were amplified (model 110F; Pacific Instruments, Concord, CA; response time <0.1 ms) and digitized by a 12-bit analog-to-digital converter (Lab Master; Scientific Solutions, Solon, OH) interfaced to a 386 cpu. During each experiment, the first 3,000 data points were collected at a rate of 100 μs − 1 ms per point, while the remaining 1,700–1,930 data points were collected at a rate of 10 ms per point.

FRAP Experimental Procedures and Data Analysis

Before each set of experiments, the FRAP instrument was stabilized for 90 min, and the attenuated and unattenuated beams were aligned and steered along the optical axis of the microscope. The recovery curves for a series of 5–8 calibration solutions were measured in quadruplicate before and after every set of experiments to provide an internal standard and to ensure that beam drift did not occur. The calibration solutions, which consisted of 240 μM BCECF in PBS (pH 7.4) containing sucrose (0–540 g/l), yielded macroscopic viscosities of 1.02 to 23.2 cP as measured by a Cannon-Fenske viscometer (models 50 and 100; Cannon Instru. Co., State College, PA); measured viscosities were in close agreement with data in the CRC handbook (Weast, 1986). FRAP measurements were performed on calibration solutions of 2–50-μm thickness prepared by depositing a defined microliter volume of solution between an 18-mm-diam round coverglass (above) and a larger rectangular coverglass (below). The solution spread evenly within the area of the round coverglass. Film thickness was confirmed from the z-axis translation required to focus on the upper and lower solution/glass interfaces.

Photobleaching parameters were computed as follows. In each measurement, the prebleach fluorescence, F(−), was determined from the average fluorescence over a 1-s interval prior to photobleaching. The time course of fluorescence recovery after photobleaching, F(t), was described by a 4-parameter biexponential function, $F(t) = A_1 \exp(-t/\tau_1) + A_2 \exp(-t/\tau_2)$

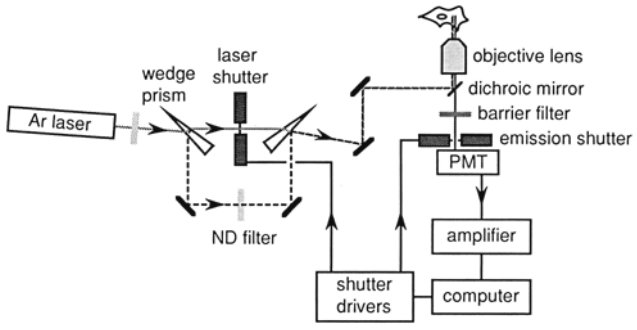

Figure 1. Schematic of FRAP apparatus designed to measure recovery times down to 5 ms. See Materials and Methods section for details.

1. *Abbreviations used in this paper*: BCECF, 2,7-bis-(2-carboxyethyl)-5-(and 6-)carboxyfluorescein; BCECF-AM, BCECF-acetoxylmethylester; FV, free volume; SE, stretched exponential.

+ $F(\infty)$, where $\tau_1 < \tau_2$. $F(\infty)$ is the (constant) fluorescence at long times after photobleaching and was determined from the average of F(t) over a 5-s interval 15–20 s after the photobleaching pulse. The F(t) curve was fitted by the successive integration procedure (On-Line Instrument Systems Inc., Jefferson, GA) for t between 7 ms after the end of the photobleaching pulse (well after the emission path shutter was opened) and 100-1000 ms. The fluorescence immediately after bleaching, F(0), was determined by extrapolating F(t) back to zero time. The percent photobleaching was thus equal to 1-F(0)/F(−); the percent recovery was equal to [F(∞)-F(0)]/[F(−)-F(0)]; and the half-time for recovery, $\tau_{1/2}$, was determined by numerically solving the equation $F(\tau_{1/2}) = [F(\infty)-F(0)]/2$. In ~10% of the FRAP studies in cells, there was a slow increase in F(t) after recovery possibly due to continued intracellular deesterification of BCECF-AM; in these experiments, F(t) was corrected using the measured rate of fluorescence increase determined from the slope of F(t) vs. t for t between 15 and 20 s.

Apparent viscosities for a given sample were determined by comparison of $\tau_{1/2}$ values for fluorescence recovery after photobleaching in the sample with $\tau_{1/2}$ values for the calibration solutions. The rationale and justification for this approach are discussed below. The diffusion coefficient in the sample relative to that in water, D/D_0, was then computed as the inverse of the apparent viscosity.

Picosecond Anisotropy Measurements

Time-resolved fluorescence polarization measurements were carried out by Fourier transform frequency-domain fluorimetry (Verkman et al., 1991). Light from a CR-4 Ar laser was impulse modulated by a Pockels cell and components of an SLM 48000 multiharmonic fluorimeter (SLM Instruments; Urbana IL) to give a 6 MHz series of 1–2 nanosecond pulses of plane-polarized light. ~4% of the light was split to a reference photomultiplier, while the main beam was steered into an inverted epifluorescence microscope and reflected by a 510-nm dichroic mirror for sample excitation through a 40× quartz objective (glycerol immersion, numerical aperture 0.65; Leitz). The beam diameter at the focal plane could be set between 1 μm and ~25 μm. Emitted fluorescence passed through the dichroic mirror, a GG530 barrier filter (Schott Glass, Duryea, PA), and a Glan-Thompson calcite polarizer that could be rotated through 90°. Polarizer alignment, G-factor corrections, and calibration with standards were carried out as described previously (Dix and Verkman, 1990; Fushimi et al., 1990). Differential phase angles and modulation ratios were measured at 35–40 discrete harmonics of the 6 MHz repetition frequency by cross-correlation multi-harmonic detection. The fluorescence from unlabeled cells was <2% of that from BCECF-loaded cells. Phase and modulation data were fitted by a non-linear least-squares procedure (Calafut et al., 1989) to a two-component anisotropy-decay model, $r(t) = g_1 \exp(-t/\tau_{1c}) + (1-g_1)\exp(-t/\tau_{2c})$, where τ_{1c} and τ_{2c} are the shorter and longer rotational correlation times, respectively, and g_1 is the fractional amplitude corresponding to τ_{1c}. In practice, g_1 represents the fraction of unbound (more rapidly rotating) fluorophore, and $(1-g_1)$ represents the fraction of bound (more slowly rotating) fluorophore. The BCECF rotational diffusion coefficient in a given sample relative to that in water, $(D/D_0)_{rot}$, was determined from the ratio of τ_1 measured in buffer to that measured in the sample (Fushimi and Verkman, 1991).

Binding and Stopped-flow Polarization Measurements

Both the extent and the kinetics of probe binding to intracellular structures will enter into the theoretical model developed in the next section. The methodology used to characterize these quantities was as follows.

The extent of BCECF binding to cytoplasmic components was determined by picosecond anisotropy measurements, as described above, and by confocal microscopy. For the latter measurements, a monolayer of 3T3 fibroblasts was permeabilized with 40 μg/ml digitonin for 30 min at 5°C and equilibrated with 100 μM BCECF acid in PBS for 15 min at 23°C. BCECF fluorescence in cell cytoplasm and the adjacent solution was measured by confocal microscopy (Technical Instruments, San Francisco, CA; 100× objective, 0.6 μm measured z-axis resolution). Binding was determined from the ratio of intracellular to extracellular fluorescence, corrected for the non-aqueous cell volume of ~20%.

The kinetics of BCECF binding in a 10% suspension of fibroblast cytoplasm and in a 5% albumin solution was determined by stopped-flow fluorescence polarization using a Hi-Tech SF51 apparatus. The method exploits the fact that steady-state fluorescence polarization (or anisotropy) increases as probe binds. Equal volumes of a 100 μM BCECF solution and a cytoplasm or albumin solution were mixed in <1 ms in a stopped-flow apparatus. The time course of fluorescence (480-nm excitation, >515 nm emission) was measured at a rate of 0.1 ms/point. To determine the time course of steady-state fluorescence anisotropy, the incident light was vertically polarized and the emitted fluorescence was measured through vertically and horizontally oriented analyzing polarizers.

Results

Theory for Slowed Diffusion in Cytoplasm

The purpose of this mathematical section is to provide a framework for the analysis of translational diffusion data in cell cytoplasm. It is assumed that cell cytoplasm consists of an aqueous fluid-phase compartment bathing a matrix of mobile and immobile particles that are much larger than the water molecules and small solutes. It is further assumed that three independent factors act to decrease the diffusion coefficient of a small solute in cytoplasm (D) relative to that in water (D_0),

$$D/D_0 = F_1(\eta) \cdot F_2(D_u, \{D_{b,i}, f_{b,i}\}) \cdot F_3(\{n_i, V_i\}) \quad (1)$$

where F_1, F_2, and F_3 are defined below.

The function $F_1(\eta)$ describes the slowing of net solute translation due to an increase in true fluid-phase cytoplasmic viscosity. Such an increase would reflect some solute-induced perturbation in solvent structure, which need not be specified. The functional form for F_1 follows from the reciprocal relationship between the diffusion coefficient and the viscosity, and can be written

$$F_1(\eta) = \eta_o/\eta \quad (2)$$

where η_0 is the viscosity of water, and η is the true fluid-phase microviscosity of cytoplasm. The fluid-phase viscosity η can be obtained from measurements of solute rotational dynamics, or potentially of short-range solute translational dynamics. The fluid-phase viscosity cannot be obtained from measurements of macroscopic cytoplasmic viscosity; indeed, the macroscopic viscosity can be many times greater than the fluid-phase viscosity (Furukawa et al., 1991; Scalettar and Abney, 1991). Eq. 2 predicts that if the fluid-phase viscosity increased by a factor of 2, D/D_0 would decrease by a factor of 2.

The function $F_2(D_u, \{D_{b,i}, f_{b,i}\})$ describes the net slowing of solute translation due to transient binding of solute molecules to cytoplasmic structures. For the simplest case in which there is solute binding only to one macromolecular species, the measured FRAP diffusion coefficient has been shown to be a linear combination of the diffusion coefficients for the bound and unbound solute, weighted by the appropriate mole fractions (Elson and Qian, 1989; Elson and Reidler, 1979; Jähnig, 1981; Koppel, 1981). This expression can be generalized to describe multiple bound species; the form for F_2 is taken as the ratio of the weighted diffusion coefficient of the bound and unbound solute to the diffusion coefficient of the unbound solute. If D_u is the diffusion coefficient of unbound solute, $D_{b,i}$ the diffusion coefficient of the *ith* bound solute, and $f_{b,i}$ the fraction of total solute bound to component i, then

$$F_2(D_u, \{D_{b,i}, f_{b,i}\}) = f_u + \sum_i (D_{b,i}/D_u) f_{b,i} \quad (3a)$$

where

$$f_u + \sum_i f_{b,i} = 1 \quad (3b)$$

It is assumed in Eq. 3 that the kinetics of solute binding and

unbinding is fast compared to the characteristic time for translational diffusion in a FRAP experiment. In the FRAP studies described below, Eq. 3 applies for submillisecond binding kinetics. For a simple situation in which 50% of the solute is unbound and 50% is bound at any instant to immobile intracellular structures ($f_u = 0.5$, $\{D_{b,i}\} = 0$), Eq. 3 predicts that D/D_o would decrease by a factor of 2.

The function F_3 ($\{n_i,V_i\}$) describes the slowing of solute translation due to collisional interactions with cytoplasmic structures, where in general there are n_i structures of type i, each having volume V_i. Two theories have been used to describe the effects of "volume occlusion" by mobile obstacles on diffusion: a stretched-exponential (SE) model (Furukawa et al., 1991; Phillies, 1989) and a free-volume (FV) model (Fujita, 1961; Furukawa et al., 1991; Landry et al., 1988). The SE model has been used to describe the diffusion of relatively large, Brownian particles, whereas the FV model has been used to describe solvent diffusion. Because BCECF is a small (nearly solvent-sized) solute, its motion can be satisfactorily described by both models. We apply both models to demonstrate model independence of the results.

The stretched-exponential model was initially developed to give a good empirical fit to diffusion data in crowded media. Recently, it has been shown that an SE equation can be derived theoretically. The SE model has been found to fit diffusion data well over a wide range of solute and occluding molecule sizes (Phillies, 1989), and has been elegantly used to describe the diffusion of large solutes in cell cytoplasm (Hou et al., 1990). For a single class of obstacles, the SE model predicts

$$F_{3,SE}(n_i,V_i) = \exp\left[-\alpha\,(n_iV_i)^{\nu}\right] \quad (4)$$

where n_iV_i is the volume fraction occupied by the occluding molecule, and the prefactor α and the exponent ν are scaling parameters. The values of α and ν can be determined empirically by fitting Eq. 4 to data, and they can be calculated independently from theory. For small solutes, ν is usually found to be near unity (Furukawa et al., 1991), while α depends on the concentration units.

In contrast, the free-volume model was derived from a molecular description of diffusion. The FV model is based on the assumption that solute diffusion in crowded media is rate-limited by the availability of "free-volume," i.e., volume sufficiently devoid of obstacles that it can be occupied by solute. The diffusion coefficient is assumed to follow an Arrhenius equation in which the (model-dependent) activation energy reflects the probability of finding appropriate free-volumes. A successful and simple formulation of the FV model was derived by Fujita (1961). For a single class of obstacles, the FV model predicts

$$F_{3,FV}(\varphi) = \exp\left[\frac{-B_d\beta(T)\,(\varphi_0 - \varphi)}{[f(0,T) + \beta(T)\varphi_0]\,[f(0,T) + \beta(T)\varphi]}\right] \quad (5)$$

where φ is the free-volume fraction of solvent, φ_o is φ in the absence of obstacles, f(0,T) is the temperature-dependent free-volume in the absence of solvent, $\beta(T)$ describes the free-volume difference between solvent and obstacles (in the appropriate reference states), and B_d describes the minimum free volume required for solute displacement. f(0,T) and $\beta(T)$ generally have small, positive values, and B_d and φ_0 are taken to be unity. Although they have physical significance, FV parameters are usually determined by parameter regression, rather than by independent experiment.

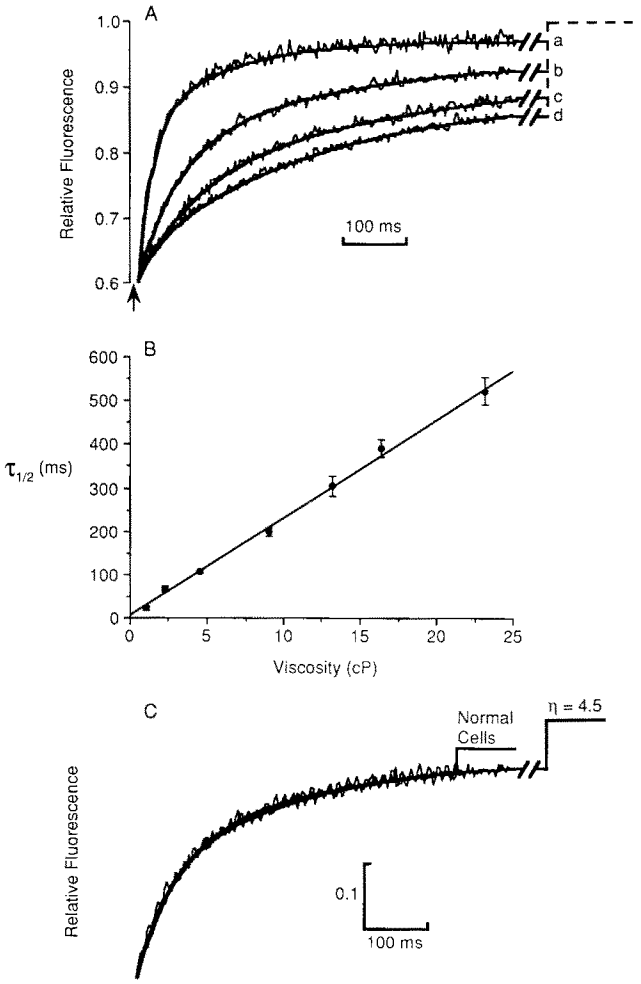

Figure 2. Validation of diffusion coefficient measurement. (*A*) Photobleaching recovery curves for solutions consisting of 240 μM BCECF in PBS containing 0–49% (wt/wt) sucrose to give viscosities of 1.02 (*a*), 4.5 (*b*), 9.1 (*c*), and 13.3 (*d*) cP. Sample thickness was 5 μm. The beginning of the photobleaching pulse is indicated by the arrow; at this time a shutter in the emission path was closed. The smooth curves through the data were obtained by biexponential regression. The dashed horizontal line denotes the value of $F(\infty)$. (*B*) Dependence of recovery half-times ($\tau_{1/2}$) on solution viscosity (η). Data from a series of calibration solutions (mean ± SEM, $n = 4$) are shown with a fitted line. (*C*) Photobleaching recovery curves for the 4.5 cP calibration solution and normal cells (23°C, isosmotic volume), demonstrating that both follow the same biexponential time course. The cell data were overlaid onto the calibration data by rescaling the associated ordinate and abscissa, while leaving the exponential amplitudes and time constants (which determine curve shape) unchanged.

Validation of Diffusion Coefficient Measurement by FRAP

The quantitative determination of BCECF diffusion coefficients in the aqueous phase of cell cytoplasm was based on the comparison of photobleaching recovery curves in cells with those in calibration solutions. Consistency in cell data therefore hinges critically on consistency in calibration data. Fig. 2 *A* shows original recovery curves for calibration solutions consisting of BCECF and various sucrose concentrations in PBS, giving viscosities between 1.02 and 13.3 cP. The intensity of the photobleaching beam was set to maintain the percent photobleaching in the range 25–45%. The

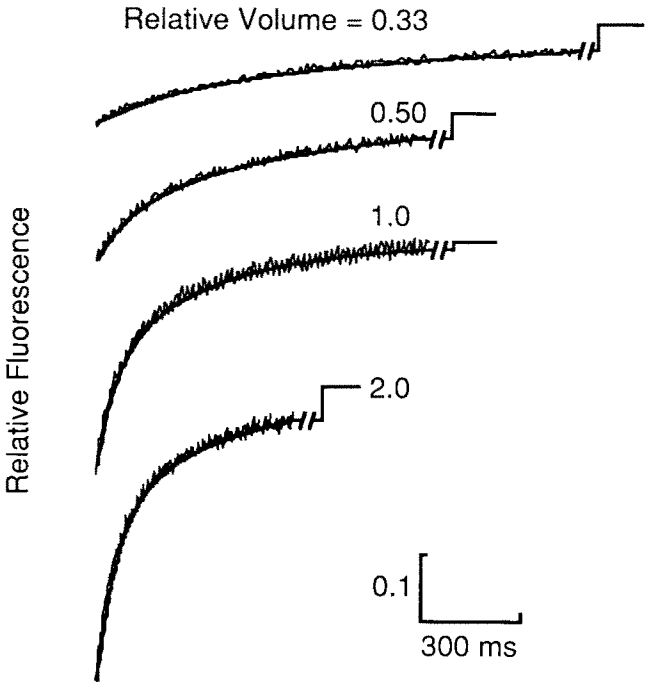

Figure 3. Effects of changes in cell volume on fluorescence photobleaching recovery curves for BCECF-labeled Swiss 3T3 fibroblasts. Cell volume was adjusted after BCECF labeling by incubating cells in media of various osmolarities. Hypoosmotic media were made by addition of sucrose to PBS; hyperosmotic media were made by dilution of PBS. Recovery curves are shown for control cells (23°C, isosmotic volume), and cells at 0.33, 0.5, and 2 times isosmotic volume.

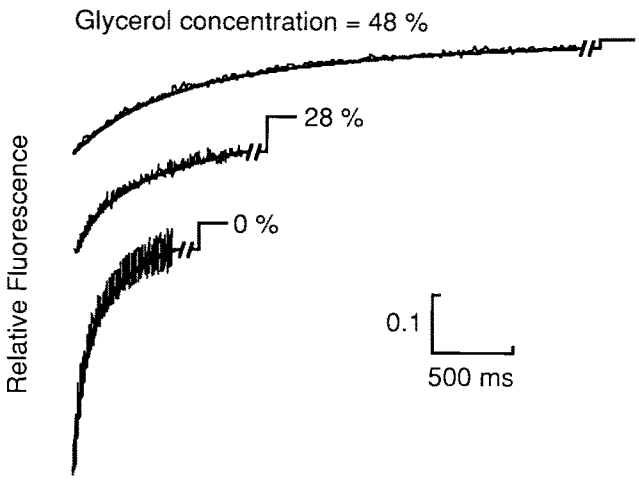

Figure 4. Effects of changes in aqueous-phase viscosity on fluorescence photobleaching recovery curves for BCECF-labeled Swiss 3T3 fibroblasts. Aqueous-phase viscosity was adjusted following BCECF labeling by incubating cells in media containing various concentrations of glycerol for 15 min at 23°C. Media were made by addition of glycerol to PBS; ionic strength was maintained at 300 mM by addition of NaCl. Recovery curves are shown for control cells (23°C, 0% glycerol), and cells in 28 and 48% (wt/wt) glycerol.

fluorescence at long times after photobleaching, F(∞), was nearly equal to that before photobleaching, F(−), indicating that all of the BCECF was mobile. In a total of 188 FRAP measurements made on calibration solutions, the percent recovery was 98 ± 1% (SEM). As solution viscosity increased, the rate of recovery decreased.

The half-time ($\tau_{1/2}$) for recovery provided a quantitative measure of the recovery rate. Because a rigorous theoretical description of the recovery-curve shape would be very complicated and has not yet appeared in the literature (see Discussion), a functional form for the recovery curve shape was chosen empirically. Although a monoexponential function did not fit the data well, a biexponential function fit the data very well as shown by the fitted curves in Fig. 2 *A*. Plots of residuals showed no systematic deviation of experimental data from the biexponential fit. In addition, the shape of the biexponential curve was nearly the same in all experiments as indicated by the similar ratios of exponential time constants. The invariance of recovery curve provides direct justification for the use of $\tau_{1/2}$ as a single parameter measure of recovery rate. Fig. 2 *B* shows a linear relationship between $\tau_{1/2}$ and viscosity for a set of calibration solutions. Although the slope of this calibration plot varied from day to day because of slight variations in beam profile and alignment (slope 21 ± 4.2 ms/cP, SD, n = 6), the slope generally changed by <20% from the beginning to the end of a 6 h set of measurements.

Since Gaussian beams diverge with distance from the focal plane, diffusion coefficients can, in principle, depend on cell thickness. However, for the 16× objective used here, the Rayleigh range (i.e., half the distance over which the beam radius remains within ~40% of its minimum value) is quite large, ~50 μm. Not surprisingly, measured $\tau_{1/2}$'s did not increase as the objective focal point was positioned up to 10 μm above or below the center of a thin (5 μm) calibration sample, or as sample thickness was increased from 2 to 50 μm. Since the maximum thickness of the 3T3 fibroblasts is <2 μm, incident beam divergence is not important in our experiments. The possible dependence of diffusion coefficient on beam spot size in considered in the Discussion.

Taken together, the findings above establish a rigorous basis for the interpretation of photobleaching curves obtained in cell cytoplasm.

FRAP Experiments in Cells

Photobleaching experiments were conducted using a 3-μm radius beam spot, which covers <1% of the area of a Swiss 3T3 fibroblast (Luby-Phelps et al., 1987). The beam was positioned to photobleach cytoplasm in an area not directly adjacent to the nucleus or cell edge. No more than one photobleaching experiment was performed on a single fibroblast. Cell experiments were calibrated using 5-μm thick standard solutions; the validity of this approach is demonstrated in Fig. 2 *C*, in which it is shown that recovery curves follow identical biexponential time courses in calibration solutions and cells. Figs. 3 and 4 show original recovery curves obtained from fibroblasts under a variety of conditions. For a fixed bleaching intensity, the percent bleaching increased with decreasing cell volume and decreasing glycerol concentration. However, the associated recovery times are independent of percent bleaching for the relatively shallow bleaching depths employed, as determined in separate experiments on calibration solutions and cells. Effective cytoplasmic viscosities derived from a series of measurements are summa-

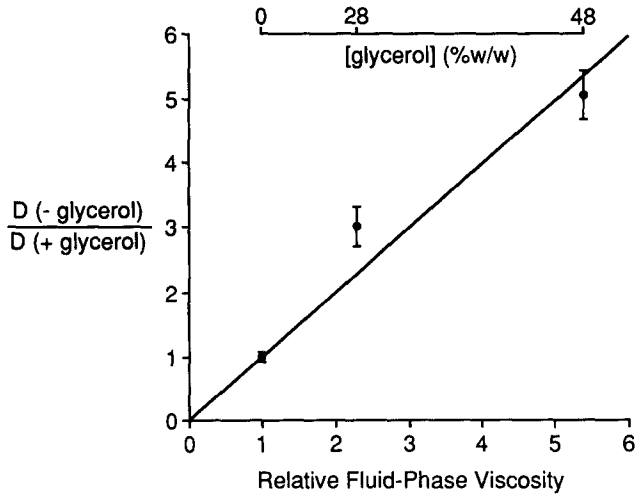

Figure 5. Slowing of BCECF translation in fibroblasts bathed in buffers containing glycerol. BCECF translational diffusion was measured by FRAP. The ordinate (mean ± SEM) is the ratio of the BCECF diffusion coefficient in control cells (−glycerol) to that in cells bathed in 28 or 48% glycerol (+glycerol). The abscissa is the viscosity (relative to water) corresponding to each glycerol concentration. Data are mean ± SEM for 13–17 measurements.

rized in Figs. 5 and 6 *A* (see below). The vast majority of BCECF was mobile in cell cytoplasm as shown by percent recoveries of >90%. In cells bathed in PBS at 23°C, the ratio of the BCECF diffusion coefficient in cytoplasm to that in water (D/D_o) was 0.27 ± 0.01 (SEM, n = 24). The distribution of D/D_o values was unimodal without any systematic dependence on the time between BCECF loading and measurement, cell passage number, or cell density. D/D_o was strongly influenced by changes in cell volume (Figs. 3 and 6 *A*) or addition of glycerol to the bathing medium (Figs. 4 and 5). In the following sections, the results of these experiments and others will be used to characterize systematically the factors that slow BCECF diffusion in cytoplasm based on the theoretical considerations described in the previous section.

Slowed BCECF Diffusion in Cytoplasm: I. Fluid-phase Viscosity

The measurement of time-resolved anisotropy provides independent information about the rotation of bound and unbound fluorophore. Moreover, because the rotation of small solutes is not hindered by collisional interactions with intracellular structures when the spacing between structures is much larger than the solute diameter (Drake and Klafter, 1990), the fluid-phase viscosity can be estimated from the rotational diffusion coefficient of the unbound BCECF. Time-resolved anisotropy was measured in BCECF-labeled fibroblasts under the conditions used for FRAP measurements as described in Materials and Methods. In four sets of control cells bathed in isosmotic buffer, BCECF rotational correlation times, τ_{1c} and τ_{2c}, were 290 ± 12 ps and 12 ± 3 ns, respectively; the fraction of (bound) BCECF with the longer correlation time was 0.19 ± 0.02. In PBS, a single rotational correlation time of 226 ps was measured. These results are in agreement with previous measurements made under similar conditions (Fushimi and Verkman, 1991). At isosmotic cell volume, the relative diffusion coefficients for

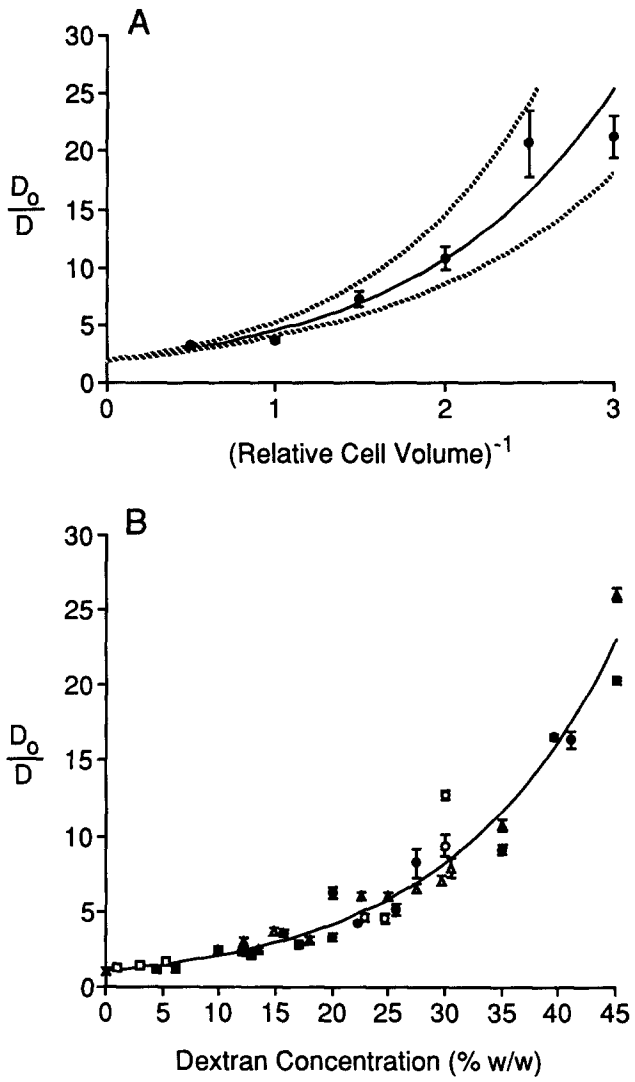

Figure 6. Slowing of BCECF translation due to volume occlusion. (*A*) D_0/D for BCECF-loaded 3T3 fibroblasts measured as a function of relative cell volume. Data are mean ± SEM for three to seven measurements. The cell data were fitted to the SE and FV models by a least-squares procedure that fixed the parameters derived in *B* and floated as a fitting parameter the factor that converts inverse cell volume to dextran concentration. The value of this conversion factor corresponding to an ordinate value of 1 in (*A*) gives the "effective percentage dextran" associated with isosmotic conditions. The derived effective dextran concentration is 13%; substituting this value into the SE and FV models gives F_3 = 0.40. The solid line indicates the fit to the cell data obtained by this procedure; the dashed lines indicate the values associated with a 15% error in the calculated value for the effective percentage dextran. The measured values all lie well within the 15% error envelope, and we thus estimate the error in the calculated value of F_3 to be ~10% (*B*) D_0/D for 100 μM BCECF in PBS solutions containing the indicated percentages (wt/wt) of dextrans of 10 kD (○), 39 kD (●) 66 kD (△), 82 (▲), and 2,000 kD (■). Additional values of D_0/D are given for agarose gels (□) and PBS alone (x; no dextran or agarose). Data were fitted to the SE and FV models; fitted parameters were: α = 0.058 and ν = 1.06 (SE model, Eq. 4) and $B_d \equiv 1$, f(0,T) = 0.0034, and β(T) = 0.015 (FV model, Eq. 5). Errors in fitted parameters probably range from 5 to 15% (Furukawa et al., 1991). The curve is the fit to the SE model; the fit to the FV model is virtually superimposable (not shown).

BCECF rotation and translation were 0.78 ± 0.03 and 0.27 ± 0.01. As cell volume increased from 0.33 to 2 times isosmotic volume, the relative rotational diffusion coefficient remained nearly constant (0.76–0.79), while the relative translational diffusion coefficient increased from 0.047 to 0.32 (Figs. 3 and 6 *A*). Thus rotation in the cytoplasm is less hindered and less sensitive to changes in cell volume than is translation.

To confirm the sensitivity of BCECF rotation to fluid-phase cytoplasmic viscosity and to test the assumption that F_1 is independent of F_2 and F_3 (see Theory section), BCECF translation and rotation were measured in cells equilibrated with 28 and 48% glycerol. These glycerol concentrations increase the macroscopic viscosity of aqueous buffers by 2.3- and 5.4-fold (Weast, 1986). As expected, the BCECF rotational diffusion coefficient (obtained from τ_{1c} measurements) decreased by approximately two- and fivefold, confirming the sensitivity of the anisotropy decay measurement. Figs. 4 and 5 show the effect of glycerol addition on the BCECF translational diffusion coefficient. The slope (0.98) of the best-fit line through the data in Fig. 5 demonstrates that the BCECF translational diffusion coefficient is nearly halved for each doubling of fluid-phase viscosity. The parallel increase in fluid-phase viscosity and BCECF translational recovery time provides direct support for the assumption that F_1 is independent of F_2 and F_3.

In summary, our data indicate that fluid-phase cytoplasmic viscosity differs to a small but significant extent from the viscosity of water. Inserting the viscosity data into Eq. 2 gives $F_1 \sim 0.78 \pm 0.03$.

Slowed BCECF Diffusion in Cytoplasm: II. Binding

The slowing of BCECF diffusion due to binding depends on the fraction of bound BCECF in cytoplasm, the mobility of bound BCECF, and the kinetics of binding. The fraction of bound BCECF was measured by two methods. First, the fractional anisotropy loss due to rapid BCECF rotation, 0.81 ± 0.01, provides a direct measure of the fraction of BCECF that rotates freely. These data suggest that 19% BCECF is bound, assuming that there is no rapidly rotating "weakly bound" BCECF (see Discussion). As cell volume changes from 0.33 to 2 times isosmotic volume, there is little change in the percentage of bound BCECF (range 18–21%). Second, the fraction of bound BCECF was estimated by Nipkow wheel confocal microscopy in digitonin-permeabilized cells that were equilibrated with 100 μM BCECF (acid, not acetoxymethylester form). BCECF intensity was measured in cells and in 2-μm-thick films of the BCECF solution used for equilibration. In four experiments, the ratio of intracellular to extracellular BCECF was 1.02, indicating that ~20% (corrected for cell aqueous volume) of intracellular BCECF is bound.

The translational mobility of bound BCECF was estimated by assuming that dye binds to cellular protein and thus diffuses like cellular protein. In previous FRAP studies (Jacobson and Wojcieszyn, 1984; Kreis et al., 1982), the cytoplasmic diffusion coefficients of native and exogenous proteins ranging in size from 12 to 440 kD were found to be 50-1,000-fold smaller than that measured here for BCECF. This result, plus the fact that some dye probably binds to truly immobile structures, suggests that the ratio D_b/D_u is very close to zero.

An attempt was made to estimate the mobility of bound fluorophore by reacting intracellular proteins non-selectively with carboxyfluorescein succinimidyl ester. Cells were hypotonically loaded with 500 μM carboxyfluorescein succinimidyl ester for 15 min and then incubated at 37°C in PBS for 60 min. FRAP data obtained from the labeled cells showed small percent bleaching relative to data obtained for aqueous or intracellular BCECF; the fluorescence recovery had a complex multi-exponential time course. The results were difficult to interpret because: (*a*) free dye apparently was considerably more bleachable than bound dye, and thus the recovery curve was dominated by the diffusion of unbound dye molecules, and (*b*) the intracellular distribution of the covalently bound dye, as determined by fluorescence microscopy, was quite different from that of the non-covalently bound BCECF.

The kinetics of BCECF binding to intracellular components was estimated by stopped-flow fluorescence polarization as described in Materials and Methods. BCECF binding to a 10% cytoplasmic homogenate and to a 5% albumin solution gave a measurable increase in polarization. 85–90% of the increased polarization occurred within the instrument dead time of 1.5 ms; ~80% of the remaining increase in polarization had a half-time of 3–5 ms. These data confirm that the binding and unbinding of BCECF occur on a time scale much faster than the half-times for photobleaching recovery.

In summary, the submillisecond BCECF binding kinetics justifies the use of Eq. 3 to describe binding effects. Taken together with the very low mobility of bound dye, Eq. 3 gives $F_2 \sim 0.81 \pm 0.01$.

Slowed BCECF Diffusion in Cytoplasm: III. Collisional Interactions

The dependence of D/D_0 on cell volume provides information that can be used to evaluate the effects of collisional interactions on BCECF translational diffusion. Because BCECF rotational diffusion and binding are influenced little by changes in cell volume as shown above, the large effects of cell volume on translational diffusion are due mainly to changes in the fraction of intracellular volume occupied by the cytomatrix.

The effects of "volume occlusion" by mobile obstacles were investigated empirically by measurement of BCECF diffusion in PBS solutions containing dextrans of different size and composition. Separate studies of anisotropy decay and binding showed little binding of BCECF to dextran and little change in aqueous-phase viscosity with increasing dextran concentration. Fig. 6 *B* shows that D_0/D increases nonlinearly as the solution volume occupied by dextran increases. The dependence of D_0/D on percentage dextran was independent of dextran size in the range 10–2,000 kD, in general agreement with results in the literature on the diffusion of small solutes in solutions containing much larger occluding solutes (Blum et al., 1986; Furukawa et al., 1991). The data fitted well to both the stretched-exponential and free-volume models as described in Theory.

The effects of "volume occlusion" by immobile obstacles were also investigated empirically. FRAP experiments were performed in 50-μm-thick films of 1, 3, and 5% low-gelling temperature agarose gels containing 500 μM BCECF in PBS. The D_0/D values given in Fig. 6 *B* (filled circles) were

in agreement with the results for equivalent dextran percentages. Unfortunately, gels with agarose concentrations greater than 5% are difficult to prepare and were not studied. However, the fact that BCECF diffusion is not sensitive to dextran size (and hence dextran mobility) suggests that obstacle mobility is much less important than obstacle concentration in determining D/D_0, at least for obstacles with sizes >10 kD. Hence, the dextran data probably provide an adequate model for the effects of volume occlusion on BCECF translation.

Fig. 6 *A* shows the relationship between D_0/D for BCECF translation and the reciprocal cell volume, which is assumed to be proportional to the concentration of the cytomatrix. The data were fitted to the stretched-exponential and free-volume models using parameters from Fig. 6 *B* and taking the percentage occluded volume (under isosmotic conditions) as a floating parameter. The data were fitted well when 13% of isosmotic cell volume is effectively occupied by occluding molecules. Because the majority of occluding molecules in cell cytoplasm are predicted to be in the 10–2,000-kD size range, the dextran solutions provide a reasonable model for cell cytoplasm. From the data in Fig. 6 *B*, 13% dextran gives an F_3 value of 0.40 ± 0.04.

Composite Effects of F_1, F_2, and F_3

The product of F_1, F_2, and F_3 determined independently above is 0.25 ± 0.03. This value is in good agreement with the D/D_0 of 0.27 ± 0.01 measured for BCECF translational diffusion in cell cytoplasm.

Additional Cell Experiments with a Smaller Photobleaching Spot Size

Some cell experiments were performed using a 100× objective (oil immersion, numerical aperture 1.3; Nikon Inc., Garden City, NY) with a 0.4-μm beam radius. FRAP experiments employing the 100× objective required special technical considerations. First, there was significant dye rearrangement during the 2–3 ms bleaching time, making the effective bleached area much larger than the beam radius. However, the use of standard solutions obviated the need for precisely characterizing the bleached area. Second, the bleach and probe beams generated by the 100× objective diverge substantially. However, we found that $\tau_{1/2}$ did not increase as the objective focal point was positioned up to 2 μm above or below the center of a thin (5 μm) calibration sample, or as sample thickness was increased from 0 to 5 μm. Beam divergence therefore did not affect our experiments on the <2-μm-thick 3T3 fibroblasts. For these experiments, the standard curves were again linear, but the recovery times were significantly smaller (slope of calibration plot as in Fig. 2 *B* = 3.5 ± 0.7 ms/cP, SD, n = 6). Experiments on control cells yielded D/D_0 = 0.24 ± 0.01 (SEM, n = 55, 23°C) at isosmotic volume. The glycerol experiments (as in Fig. 5) gave D(−glycerol)/D(+glycerol) of 1.0, 2.1, and 5.3 for cells incubated in 0, 28, and 48% glycerol. The cell volume experiments (as in Fig. 6 *A*) gave D_0/D of 3.0, 4.2, 13, and 23 for cell volumes of 2, 1, 0.5, and 0.33 times isosmotic volume. The latter experiments imply that F_3 = 0.44, corresponding to an equivalent dextran concentration of 13%. The product of F_1, F_2, and F_3 is 0.28 ± 0.03, in good agreement with the value of 0.24 ± 0.01 (obtained with the 100× objective).

Discussion

The goals of this study were to measure the translational mobility of a small solute in cell cytoplasm and to construct a consistent physical model of the factors that hinder solute translation. A small solute, rather than a labeled dextran or ficoll, was chosen as the probe molecule so that the results would apply to small intracellular metabolites without the need to extrapolate data obtained for large probes to zero probe molecular size. The translational motion of a small solute in cell cytoplasm has not been quantified previously by photobleaching recovery techniques; because of the very fast recovery times, only a lower limit has been established for the translational diffusion coefficient of fluorescein-type probes (Jacobson and Wojcieszyn, 1984). We found that the fluorescent probe BCECF was mobile in cell cytoplasm and had short photobleaching-recovery times that yielded a translational diffusion coefficient relative to that in water (D/D_0) of 0.27 ± 0.01. This value is significantly less than unity and less than the BCECF rotational diffusion coefficient relative to that in water $(D/D_0)_{rot}$ of 0.78 ± 0.03. Theoretical analysis and experiments on model solutions and cells were carried out to explain these results and to reconcile the differences. It was concluded that the low D/D_0 for BCECF translation could be quantitatively attributed to the combination of three independent factors: increased fluid-phase cytoplasmic viscosity, intacellular BCECF binding, and BCECF collisional interactions with cytoplasmic structures. Moreover, the disparity between the relative translational and rotational diffusion coefficients was found to arise because rotation is relatively insensitive to the factor that most significantly perturbs translation: collisions with occluding macromolecules. The value for D/D_0 and its physical basis have important implications for cellular processes as discussed below.

The quantitative analysis of the photobleaching recovery of a cytoplasmic probe required special considerations. A rigorous theory exists for the calculation of recovery-curve shape for the two-dimensional diffusion of a fluorophore in a spot photobleaching experiment (Axelrod et al., 1976). The theory assumes a Gaussian beam profile, perfect alignment of bleach and probe beams, no movement of unbleached dye into the bleached area during the bleaching pulse, first-order bleaching kinetics, and accurate knowledge of beam diameter. A similar theory describing the three-dimensional diffusion of fluorophore in a region illuminated by a diverging Gaussian beam does not exist. Furthermore, studies of two-dimensional systems have shown that results extracted from theory can be greatly affected by difficulties inherent in obtaining reproducible beam profiles and alignment (Barisas, 1980), bleach pulses that are short relative to the recovery kinetics (Bertch and Koppel, 1988), and purely first-order bleaching kinetics (Bjarneson and Peterson, 1991). For these reasons, our approach was to compare recovery curves for cells with curves obtained for a series of thin films of aqueous buffers having known viscosity. Recovery curves were obtained in the calibration solutions before and after every set of experiments to ensure stability of beam profile and alignment, and to provide a calibration relation for determination of apparent viscosity from recovery half-times. The use of calibration standards makes unnecessary the characterization of beam profile and alignment because the standard and samples are bleached and probed

under identical conditions. Another important design criterion was the use of a very brief bleach pulse to minimize diffusion of unbleached dye into the bleached area during the bleaching pulse. In these experiments, a 2–3 ms bleach pulse with 5,000:1 attenuation ratio for bleach-to-probe beam intensity was generally used.

Photobleaching experiments monitor diffusion over micron-scale distances. The distance probed is approximately proportional to $(\tau_{1/2})^{1/2}$, and thus the distance scale probed here with the 16× objective (3 μm) is probably about twice that probed with the 100× objective. (The characteristic distance scale monitored by the 100× objective is significantly larger than its spot size because dye moves extensively during the bleaching pulse for this objective.) The consistency between the diffusion coefficients obtained with the 16× (D/D_0 = 0.27 ± 0.03) and 100× (D/D_0 = 0.24 ± 0.03) objectives suggests that diffusion within the cytoplasm is not sensitive to distance on the micron distance scale. This observation is in accord with theoretical predictions that the diffusion coefficient should be sensitive to distance only in a regime that is comparable to the obstacle spacing (Pusey and Tough, 1985; Scalettar and Abney, 1991). The distance scale studied here is typical of that studied in spot photobleaching experiments of cytoplasmic diffusion (1.5–6.0 μm; Jacobson and Wojcieszyn, 1984; Kreis et al., 1982; Luby-Phelps and Taylor, 1988; Luby-Phelps et al., 1986, 1987, 1988; Wojcieszyn et al., 1981) and smaller than that studied in pattern photobleaching experiments (11.8 μm to one-half cell size; Blatter and Wier, 1990; Wang et al., 1982).

The rotational motion of small fluorophores was described by an anisotropy decay model containing two rotational correlation times that differed by a factor of >20. From studies of aqueous buffers containing glycerol to increase viscosity and proteins to bind fluorophore (Fushimi and Verkman, 1991), the shorter correlation time was assigned to rotation of unbound dye and the longer correlation time to rotation of bound dye. The agreement between estimates of intracellular BCECF binding by anisotropy decay and intracellular partitioning (measured by confocal microscopy) supports the assignment of the shorter correlation time to the rotation of unbound dye. However, there are several caveats in the interpretation of anisotropy data that deserve mention. Although the two-component anisotropy decay model provided a good statistical fit to phase and modulation data as judged by χ^2 analysis, it is likely that heterogeneity exists in dye rotation associated with the short and long rotational correlation times; if the data were sufficiently well-resolved, a model containing a bimodal distribution of rotational correlation times might be superior. Furthermore, it must be recognized that the measured fluid-phase cytoplasmic viscosity is valid only in aqueous compartments to which the solute has access; no direct information is available about the possible existence and properties of compartments that exclude solutes. If compartments that exclude solute do exist, then their physical properties are probably not important for cellular enzymatic and metabolic events. However, such compartments may act as additional obstacles that will further slow solute diffusion.

The translational motion of a small solute is governed by 3 factors: the instantaneous velocity of the solute when it is in motion, the fraction of time spent in motion, and the route between initial and final positions. The first factor is determined by an impediment to motion that acts over short time (or distance) scales, i.e., viscosity. The second factor is determined by the fraction of solute molecules that are bound (not in motion) at any instant in time. The third factor is determined by the solute trajectory in space, which depends upon the nature and distribution of obstacles. It is conceptually reasonable that (to a first approximation) binding is independent of viscosity and collisions. The results of the experiments in which glycerol was added to increase fluid-phase viscosity demonstrate experimentally that viscosity is independent of binding and collisions. Finally, solute-solvent interactions, which determine the viscosity, are much stronger than solute-solute interactions, which determine the collisional effects (Pusey and Tough, 1985). Factors 1 and 3 thus influence diffusion over very different time (or distance) scales and are largely independent of one another (Pusey and Tough, 1985). The good agreement between the product of the three factors that govern BCECF diffusion in cytoplasm, as determined independently, and the observed rate of BCECF diffusion, provides further support for the separation of the overall barrier to diffusion into three independent components.

The translational motion of a small solute between an initial and a final position can be compared to the motion of an auto on a road, providing useful heuristic insight into the factors that slow solute motion. The time required for an auto to reach a target destination depends on its speed, the fraction of time it is in motion, and its route. The auto's speed (assumed to be constant when the auto is in motion) is analogous to fluid-phase solute diffusion (F_1) driven by thermal energy. The fraction of time the auto is in motion (as opposed to stopped at red lights, etc.) is analogous to intracellular binding (F_2). Finally, the auto's route is analogous to the effects of obstacles (F_3), and can include traffic congestion (fluctuations in obstacle concentration) and cul-de-sacs (dead ends among immobile obstacles).

In addition, shortcomings in the solute/auto analogy provide useful insight into the differences between driven motion and random, diffusive motion. For the auto, the driver consciously chooses both the speed and the route, and can navigate the shortest distance between two points. However, the cost of this precision is that energy must be expended. For the Brownian solute, the speed is dictated by temperature and solvent viscosity, and the route traveled is random. The random route means that the time taken to travel between two points varies, and that the solute may not reach the second point at all. However, the advantage of this imprecision is that no energy must be expended. Brownian motion thus provides a cost-effective transport mechanism useful whenever precision and timing need not be exact.

The results and analyses reported in this study have direct relevance to other studies of the dynamics of solutes in crowded biological systems. A large body of related work has focused on the determinants of the diffusion of large molecules in the cytoplasm (reviewed by Luby-Phelps et al., 1988) as well as lipids (reviewed by Blackwell and Whitmarsh, 1990) and proteins (reviewed by Jacobson et al. [1987] and Scalettar and Abney [1991]) in biological membranes. Membrane proteins provide a particularly striking example of hindered diffusion: their translation can be more than 100-fold slower in biological membranes than in dilute artificial membranes. Less than one-tenth of this decrease

can be attributed to the factor herein called F_3 (Scalettar and Abney, 1991). The present study would suggest that this is not surprising and that F_1, F_2, and F_3, only when taken together, can account for the total decrease in protein mobility in biological membranes.

In summary, there are two principle conclusions to this study. First, the translational diffusion coefficient of a small solute (BCECF) in cytoplasm relative to that in water, D/D_0, is 0.27 ± 0.01. Second, this value can be modeled as a product ($D/D_0 = F_1F_2F_3 = 0.25 \pm 0.03$) of three independent factors reflecting increased fluid-phase cytoplasmic viscosity ($F_1 = 0.78$), BCECF binding to relatively immobile cellular components ($F_2 = 0.81$), and, most importantly, collisional interactions of BCECF with cytoplasmic components ($F_3 = 0.40$). Therefore, for a small metabolite-sized solute that does not bind to cellular components, the diffusion coefficient for long-range translation would be $\sim 2 \times 10^{-6}$ cm^2/s. The characteristic times associated with solute diffusion over 10 nm, 1 μm, and 10 μm distances would thus be 80 ns, 800 μs, and 80 ms, respectively.

We wish to thank Dr. Zen Ke for help with cell culture, Dr. Nallagounder Periasamy for assistance with the time-resolved spectrofluorimetry, and Dr. Bethe Scalettar for numerous comments on the theory and manuscript.

This work was supported by grants DK43840, DK35124, and HL42368 from the National Institutes of Health and a grant from the Cystic Fibrosis Foundation. Dr. Abney was supported by training grant HL07185. Dr. Verkman is an established investigator of the American Heart Association.

Received for publication 11 March 1992 and in revised form 17 September 1992.

References

Axelrod, D., D. E. Koppel, J. S. Schlessinger, E. Elson, and W. W. Webb. 1976. Mobility measurement by analysis of fluorescence photobleaching recovery kinetics. *Biophys. J.* 16:1055–1069.

Barisas, B. G. 1980. Criticality of beam alignment in fluorescence photobleaching recovery experiments. *Biophys. J.* 29:545–548.

Bertch, M. A., and D. E. Koppel. 1988. Fluorescence redistribution after photobleaching—the effect of diffusion during bleaching. *Biophys. J.* 53: 512a (Abstract).

Bjarneson, D. W., and N. O. Petersen. 1991. Effects of second order photobleaching on recovered diffusion parameters from fluorescence photobleaching recovery. *Biophys. J.* 60:1128–1131.

Blackwell, M. F., and J. Whitmarsh. 1990. Effect of integral membrane proteins on the lateral mobility of plastoquinone in phosphatidylcholine proteoliposomes. *Biophys. J.* 58:1259–1271.

Blatter, L. A., and W. G. Wier. 1990. Intracellular diffusion, binding, and compartmentalization of the fluorescent calcium indicators indo-1 and fura-2. *Biophys. J.* 58:1491–1499.

Blum, F. D., S. Pickup, and K. R. Foster. 1986. Solvent self-diffusion in polymer solutions. *J. Colloid Interface Sci.* 113:336–341.

Bridgman, P. C., and T. S. Reese. 1984. The structure of cytoplasm in directly frozen cultured cells. I. Filamentous meshworks and the cytoplasmic ground substance. *J. Cell Biol.* 99:1655–1668.

Calafut, T. M., J. A. Dix, and A. S. Verkman. 1989. Fluorescence depolarization of cis- and trans-parinaric acids in artificial and red cell membranes resolved by a double hindered rotational model. *Biochemistry.* 28:5051–5058.

Chao, A. C., J. A. Dix, M. Sellers, and A. S. Verkman. 1989. Fluorescence measurement of chloride transport in monolayer cultured cells: mechanisms of chloride transport in fibroblasts. *Biophys. J.* 56:1070–1081.

Clegg, J. S. 1984. Intracellular water and the cytomatrix: some methods of study and current views. *J. Cell Biol.* 99(1, Pt. 2):167s–171s.

Dix, J. A., and A. S. Verkman. 1990. Mapping of fluorescence anisotropy in living cells by ratio imaging: application to cytoplasmic viscosity. *Biophys. J.* 57:231–240.

Drake, R. D., and J. Klafter. 1990. Dynamics of confined molecular systems. *Phys. Today.* 43(5):46–55.

Elson, E. L., and J. A. Reidler. 1979. Analysis of cell surface interactions by measurements of lateral mobility. *J. Supramol. Struct.* 12:481–489.

Elson, E. L., and H. Qian. 1989. Interpretation of fluorescence correlation spectroscopy and photobleaching recovery in terms of molecular interactions. *Methods Cell Biol.* 30:307–332.

Fujita, H. 1961. Free-volume model of diffusion in polymer solutions. *Adv. Polymer Sci.* 3:1–47.

Fulton, A. B. 1982. How crowded is the cytoplasm? *Cell.* 30:345–347.

Furukawa, R., J. L. Arauz-Lara, and B. R. Ware. 1991. Self-diffusion and probe diffusion in dilute and semidulute aqueous solutions of dextran. *Macromolecules.* 24:599–605.

Fushimi, K., and A. S. Verkman. 1991. Low viscosity in the aqueous domain of cell cytoplasm measured by picosecond polarization microscopy. *J. Cell Biol.* 112:719–725.

Fushimi, K., J. A. Dix, and A. S. Verkman. 1990. Cell membrane fluidity in the intact kidney proximal tubule measured by orientation-independent fluorescence anisotropy imaging. *Biophys. J.* 57:241–254.

Gershon, N. D., K. R. Porter, and B. L. Trus. 1985. The cytoplasmic matrix: its volume and surface area and the diffusion of molecules through it. *Proc. Natl. Acad. Sci. USA.* 82:5030–5034.

Hou, L., F. Lanni, and K. Ludy-Phelps. 1990. Tracer diffusion in F-actin and ficoll mixtures: toward a model for cytoplasm. *Biophys. J.* 58:31–43.

Jacobson, K., and J. Wojcieszyn, 1984. The translational mobility of substances within the cytoplasmic matrix. *Proc. Natl. Acad. Sci.* 81:6747–6751.

Jacobson, K., A. Ishihara, and R. Inman. 1987. Lateral diffusion of proteins in membranes. *Ann. Rev. Physiol.* 49:163–175.

Jähnig, F. 1981. No need for a new membrane model. *Nature (Lond.).* 289: 694–696.

Keith, A. D. 1973. Viscosity of cellular protoplasm. *Science (Wash. DC).* 183:666–668.

Keith, A. D., W. Snipes, R. J. Mehlhorn, and T. Gunter. 1977. Factors restricting diffusion of water-soluble spin labels. *Biophys. J.* 19:205–218.

Koppel, D. E. 1981. Association dynamics and lateral transport in biological membranes. *J. Supramol. Struct. Cell. Biochem.* 17:61–67.

Kreis, T. E., B. Geiger, and J. Schlessinger. 1982. Mobility of microinjected rhodamine actin within living chicken gizzard determined by fluorescence photobleaching recovery. *Cell.* 29:835–845.

Landry, M. R., Q.-j. Gu, and H. Yu. 1988. Probe molecule diffusion in polymer solutions. *Macromolecules.* 21:1158–1165.

Lepock, J. R., K. H. Cheng, S. D. Campbell, and J. Kruuv. 1983. Rotational diffusion of tempone in the cytoplasm of Chinese hamster lung cells. *Biophys. J.* 44:405–412.

Lindmo, T., and H. B. Steen. 1977. Flow cytometric measurement of the polarization of fluorescence from intracellular fluorescein in mammalian cells. *Biophys. J.* 18:173–187.

Luby-Phelps, K., and D. L. Taylor. 1988. Subcellular compartmentalization by local differentiation of cytoplasmic structure. *Cell Motil.* 10:28–37.

Luby-Phelps, K., D. L. Taylor, and F. Lanni. 1986. Probing the structure of cytoplasm. *J. Cell Biol.* 102:2015–2022.

Luby-Phelps, K., P. E. Castle, D. L. Taylor, and F. Lanni. 1987. Hindered diffusion of inert tracer particles in the cytoplasm of mouse 3T3 fibroblasts. *Proc. Natl. Acad. Sci. USA.* 84:4910–4913.

Luby-Phelps, K., F. Lanni, and D. L. Taylor. 1988. The submicroscopic properties of cytoplasm as a determinant of cellular function. *Ann. Rev. Biophys. Biophys. Chem.* 17:369–396.

Mastro, A. M., and A. D. Keith. 1984. Diffusion in the aqueous compartment. *J. Cell Biol.* 99(1, Pt. 2):180s–187s.

Mastro, A. M., M. A. Babich, W. D. Taylor, and A. D. Keith. 1984. Diffusion of a small molecule in the cytoplasm of mammalian cells. *Proc. Natl. Acad. Sci. USA.* 81:3414–3418.

Periasamy, N., H. P. Kao, K. Fushimi, and A. S. Verkman. 1992. Organic osmolytes increase cytoplasmic microviscosity in kidney cells. *Am. J. Physiol.* 263:C901–C907.

Phillies, G. D. J. 1989. The hydrodynamic scaling model for polymer self-diffusion. *J. Phys. Chem.* 93:5029–5039.

Porter, K. R. 1984. The cytomatrix: a short history of its study. *J. Cell Biol.* 99(1, Pt. 2):3s–12s.

Pusey, P. N., and R. J. A. Tough. 1985. Particle interactions. *In* Dynamic Light Scattering: Applications of Photon Correlation Spectroscopy. R. Pecora, editor. Plenum Publishing Corp., New York. 85–179.

Scalettar, B. A., and J. R. Abney. 1991. Molecular crowding and protein diffusion in biological membranes. *Comments Mol. Cell Biol.* 7:79–107.

Verkman, A. S., M. Armijo, and K. Fushimi. 1991. Construction and evaluation of a frequency-domain epifluorescence microscope for lifetime and anisotropy decay measurements in subcellular domains. *Biophys. Chem.* 40:117–125.

Wang, Y.-L., F. Lanni, P. L. McNeil, B. R. Ware, and D. L. Taylor. 1982. Mobility of cytoplasmic and membrane-associated actin in living cells. *Proc. Natl. Acad. Sci. USA.* 79:4660–4664.

Weast, R. C., Editor-in-Chief. 1986. *CRC Handbook of Chemistry and Physics.* 67th Edition. CRC Press, Boca Raton, Florida. pp. D-232 and D-262.

Wojcieszyn, J. W., R. A. Schlegel, E. S. Wu, and K. A. Jacobson. 1981. Diffusion of injected macromolecules within the cytoplasm of living cells. *Proc. Natl. Acad. Sci. USA.* 78:4407–4410.